



Ongoing oroclinal bending in the Cascadia forearc and its relation to concave-outboard plate margin geometry

Theron Finley^{1,2}, Kristin Morell^{1,3}, Lucinda Leonard¹, Christine Regalla⁴, Stephen T. Johnston², and Wenbo Zhang^{1,2}

¹School of Earth and Ocean Sciences, University of Victoria, 3800 Finnerty Road, Victoria, British Columbia V8P 5C2, Canada

²Department of Earth and Atmospheric Sciences, University of Alberta, 1-26 Earth Sciences Building, Edmonton, Alberta T6G 2E3, Canada

³Department of Earth Sciences, University of California, Santa Barbara, 1006 Webb Hall, Santa Barbara, California 93106, USA

⁴Department of Earth and Environment, Boston University, 685 Commonwealth Avenue, Boston, Massachusetts 02215, USA

ABSTRACT

The concave-inboard (concave toward the overriding plate) geometry of most convergent margins is considered a natural consequence of the depression of the edge of a thin spherical cap, whereas concave-outboard margin segments commonly form around indenters on the subducting plate. At the Cascadia subduction zone, the apex of a >500-km-long concave-outboard bend in the trench presently shows no obvious subduction of an indenter, but does coincide with the axis of an outboard-facing concavity in upper-plate rocks arched around the Olympic Peninsula in northwestern Washington State, USA. Here we synthesize paleomagnetic and structural data together with new analyses of Global Navigation Satellite System data to show that the upper plate at Cascadia has been folded from the Miocene to the present into an orocline with an axial trace that bisects the Olympic Peninsula. The processes that accommodate bending, which we suggest include (1) folding by flexural slip on the orocline limbs and (2) shortening, uplift, and escape within the core of the fold at the Olympic Mountains, have the combined result of relative motion of the forearc towards the arc at the core of the orocline, and sustained opposing rotations of the upper plate on the orocline limbs. We propose that oroclinal bending is promoted and maintained by along-strike variations in plate-boundary tractions resulting from the geometry of the plate interface at depth and suggest that these processes can contribute to the development of concave-outboard margins without the need for a subducting indenter.

INTRODUCTION

The geometry and shape of convergent margins and consequent variations in relative plate motion influence a number of important seismicogenic processes, including the distribution of locking on the plate interface (e.g., Wang et al., 2003) and strain partitioning between the megathrust and the overriding plate (e.g., Yu et al., 1993). The broad concave-inboard geometry of most convergent margins is considered a natural consequence of the depression of the edge of a thin spherical cap (e.g., Mahadevan et al., 2010), while syntaxis concave-outboard margin segments commonly form around a subducting indenter such as an oceanic plateau or seamount chain (e.g., Bendick and Ehlers, 2014; Marshak, 2004). Along the eastern margin of the Pacific Ocean, there are several >500-km-long concave-outboard convergent margin sections (Bolivia, Panama, and Cascadia; Fig. 1) that currently show no obvious subduction of an indenter, but do show evidence for past or

present oroclinal bending within the upper plate near the apex of the trench concavity (e.g., Silver et al., 1990; Allmendinger et al., 2005a; Johnston and Acton, 2003). In the case of the “Bolivian orocline” (BOL, Fig. 1), Global Navigation

Satellite System (GNSS) and paleomagnetic data together demonstrate that oroclinal bending has been occurring continuously since at least 26 Ma (Allmendinger et al., 2005a). These observations suggest that oroclinal bending may be an important process in the long-term evolution of concave-outboard convergent margins over long spatial wavelengths.

Here we focus on a region of the Cascadia subduction zone where, similar to the Bolivian case, the apex of a >500-km-long concave-outboard bend in the trench (Fig. 2A) appears coincident with the axis of an outboard-facing concavity in upper-plate rocks arched around the Olympic Peninsula in northwestern Washington State, USA (Fig. 2B) (Beck and Engebretson, 1982; Brandon and Calderwood, 1990; Warnock et al., 1993). We use paleomagnetic and structural data to show that oroclinal bending is responsible for the arcuate shape of these rock formations, and use geodetic data to show that the upper plate has been folding from at least the Miocene to the present into an orocline. We propose that ongoing oroclinal bending has

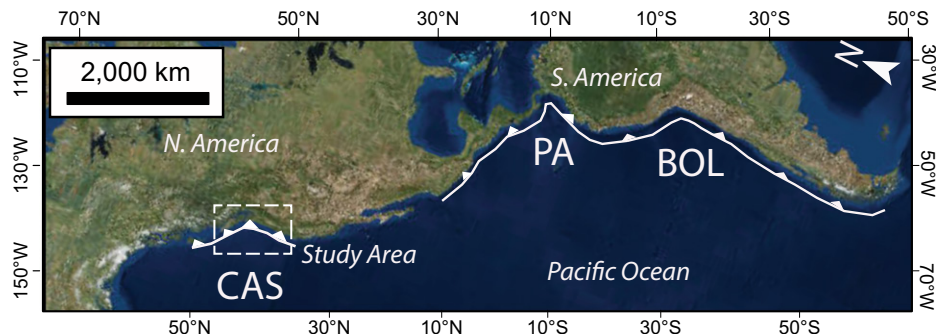


Figure 1. Convergent margins of eastern Pacific Ocean (trenches outlined in white). Cascadia (CAS), Panama (PA), and Bolivia (BOL) all display concave-outboard trench geometry and show evidence for oroclinal bending in upper plate (Silver et al., 1990; Allmendinger et al., 2005a). Imagery from ESRI DigitalGlobe (<https://www.digitalglobe.com>). Study area outlined with dashed white box.

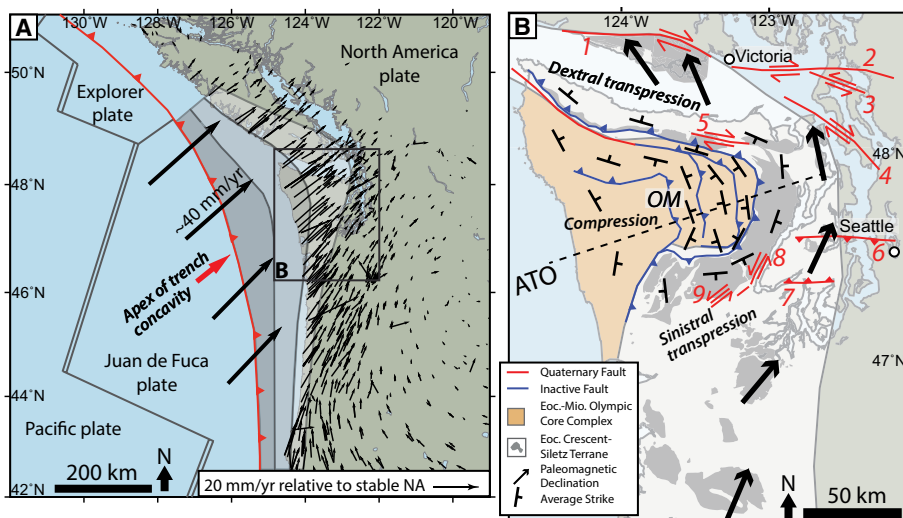


Figure 2. A: Tectonic setting of concave-outboard Cascadia subduction zone, showing Juan de Fuca–North America plate motion (thick black arrows, MORVEL model; DeMets et al., 2010) and Global Navigation Satellite System (GNSS) velocity vectors (thin arrows; error ellipses [0.43 mm/yr mean standard error] omitted for clarity) relative to stable North America (NA) (UNAVCO Plate Boundary Observatory database, <https://www.unavco.org/data/gps-gnss/data-access-methods/dai2/app/dai2.html>; McCaffrey et al., 2013). Megathrust interseismic locking pattern is from Wang et al. (2003), where locked zone is dark gray and locking decreases downdip through effective transition zone (lighter gray); B: Generalized geologic setting surrounding Olympic Mountains (OM), northwestern Washington State, USA, showing geologically defined axial trace of orocline (ATO), paleomagnetic declinations (Beck and Engebretson, 1982; Prothero et al., 2008), average orientations of foliations within 23 structural domains (see the Data Repository [see footnote 1] for details), and Quaternary-active crustal faults with modern fault kinematics shown by red arrow pairs (U.S. Geological Survey Quaternary Fault and Fold database [<http://earthquake.usgs.gov/hazards/qfaults>] unless otherwise noted): 1—Leech River fault (Morell et al., 2017; Li et al., 2018); 2—Darrington-Devils Mountain fault zone, 3—Utsalady Point fault; 4—Southern Whidbey Island fault zone; 5—Lake Creek-Boundary Creek fault (Nelson et al., 2017); 6—Seattle fault; 7—Tacoma fault; 8—Saddle Mountain fault; 9—Canyon River fault. Eoc.—Eocene; Mio.—Miocene.

led to the development of the concave-outboard geometry of Cascadia due to along-strike variations in plate-boundary tractions imposed by the geometry of the lower plate.

EVIDENCE FOR PAST AND PRESENT OROCLINAL BENDING AT CASCADIA

Paleomagnetic and Structural Constraints on Post-Eocene Bending

Inboard of the trench concavity at Cascadia (Fig. 2A), ophiolitic basalts of the Crescent-Siletz terrane form an arcuate belt around the eastern periphery of the Olympic Mountains (Fig. 2B). This arcuate pattern has long been recognized, but its origin is debated (Cady, 1975; Brandon and Calderwood, 1990; Warnock et al., 1993) and the timing of its formation has previously been restricted to the Eocene (Johnston and Acton, 2003). Oroclinal bending, where an originally linear belt is bent around a vertical axis to form a curved map pattern (Carey, 1955), predicts opposing senses of vertical-axis rotation on each orocline limb and parallelism between foliations and paleomagnetic declinations within the orocline (Eldredge et al., 1985).

Observations in the Cascadia forearc provide evidence for both of these predictions. First,

paleomagnetic declinations measured in rocks of the Eocene Crescent-Siletz terrane and the overlying Oligocene Sooke Formation (Beck and Engebretson, 1982; Warnock et al., 1993; Prothero et al., 2008) record clockwise rotation to the south of the Olympic Peninsula, compared to counterclockwise rotation to the north (Fig. 2B). These data indicate an average of 22° of post-Eocene rotation, with a reversal of rotation sense located near the axial trace of the geologically defined orocline in the Crescent-Siletz terrane (Fig. 2B). Second, structural data collected from both the Crescent-Siletz terrane and the Olympic core complex (Washington Geological Survey, 2017) reveal a systematic along-strike change shared among paleomagnetic declinations and the strike of regional foliations (Fig. 2B; Fig. DR1 in the GSA Data Repository¹). These relationships suggest that the arcuate shape of the Crescent-Siletz terrane has resulted from post-Eocene bending of an originally linear belt, as predicted by an orocline model (e.g., Eldredge et al., 1985).

¹GSA Data Repository item 2019058, Figure DR1, Table DR1, and GNSS analysis methods, is available online at <http://www.geosociety.org/darepository/2019/>, or on request from editing@geosociety.org.

Geodetic Constraints on Contemporary Bending

To test whether orocinal bending is occurring in the Cascadia forearc today, we calculated vertical-axis rotations using processed GNSS velocity data from 282 continuous sites and 641 campaign sites, with average time-series lengths of 10.3 yr and 6.5 yr, respectively (Fig. 2A; UNAVCO Plate Boundary Observatory [<https://www.unavco.org/data/gps-gnss/data-access-methods/dai2/app/dai2.html>]; McCaffrey et al., 2013). We first used an adaptive Gaussian smoothing function (Mazzotti et al., 2011) to interpolate crustal velocity across a 0.2° × 0.2° grid. Annual rotation rates were then derived by calculating the curl of the smoothed velocity field at each grid point (see the Data Repository for details).

The analysis of GNSS velocity data shows ~0.5°–2°/m.y. of contemporary rotation on each limb of the Olympic orocline, with a distinct northward transition from clockwise to counterclockwise rotation across the Olympic Peninsula (Fig. 3; Table DR1 in the Data Repository). The switch in rotation sense correlates spatially with both the reversal in rotations recorded by paleomagnetic declinations and with the geologically defined axial trace of the orocline (Fig. 2B). These spatial similarities suggest that, rather than being solely related to Eocene processes (e.g., Johnston and Acton, 2003), orocinal bending has been continuous through time, recorded in the long term (>10 m.y.) by geologic and paleomagnetic data (Fig. 2B), and in the short term (>10 yr) by the GNSS vertical-axis rotations (Fig. 3). Moreover, although the GNSS velocity field of the Cascadia forearc is strongly influenced by interseismic strain due to megathrust locking (e.g., Wang et al., 2003), the correlation between short-term and long-term vertical-axis rotations in the forearc implies that a portion of upper-plate crustal strain occurring during the megathrust interseismic period results in permanent crustal deformation.

OROCLINAL BENDING PROCESSES AT CASCADIA

Based on our synthesis of paleoseismic, geodetic, geomorphic, and thermochronologic data, we suggest that orocinal bending at Cascadia is accommodated via a combination of flexural slip (Donath and Parker, 1964), orthogonal flexure (Bobillo-Ares et al., 2000), and fold axis-parallel extrusion (Dietrich, 1989), wherein transpression with opposite slip sense occurs on the orocline limbs and compression occurs within the orocline core (Fig. 2B). Paleoseismic data show that Quaternary fault kinematics are dominantly right lateral-transpressional to the north of the orocline and left lateral-transpressional to the south (e.g., Nelson et al., 2017). At the core of the orocline, the Olympic Mountains exhibit upper-plate shortening (Mazzotti

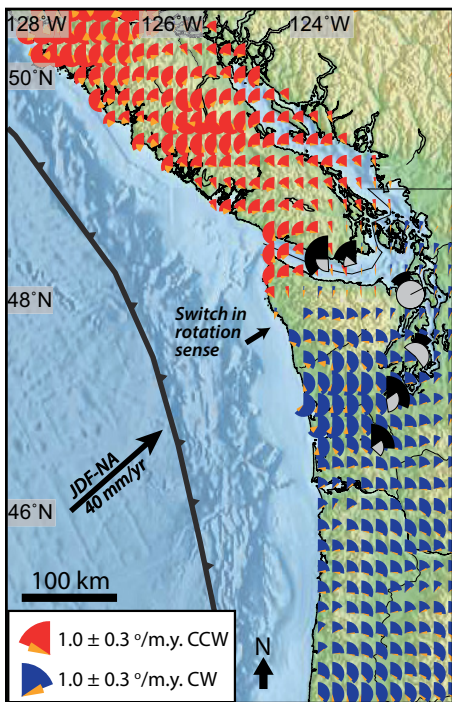


Figure 3. Vertical axis rotations derived from Global Navigation Satellite System (GNSS) velocities in Figure 2A. Red and blue wedges indicate sense and magnitude of rotation; small orange wedges show 1σ uncertainty. Black and gray wedges show rotations (and uncertainties) derived from paleomagnetic data, assuming bending initiated at ca. 18 Ma, the onset time of Olympic Mountain uplift (Brandon et al., 1998). JDF-NA—Juan de Fuca–North America plate motion; CCW—counterclockwise; CW—clockwise.

et al., 2002), lateral material escape (Nelson et al. 2017), and high rates of uplift and incision (Pazzaglia and Brandon, 2001)—processes that are expected within the core of an actively developing fold.

We suggest that the geometry of the subducting slab, and resulting spatial variations in plate-boundary tractions, are key factors in promoting and maintaining oroclinal bending at Cascadia. In map view, the axial trace of the orocline is subparallel to the hinge of a broad arch (upward convexity) in the subducting slab (Fig. 4). The gentler subduction angle at this slab arch hinge leads to a locally lower thermal gradient along the plate interface and a consequently wider locked zone beneath the Olympic Peninsula (Fig. 2A) (e.g., Wang et al., 2003). This configuration results in GNSS crustal velocities that are greatest near the orocline core (~20 mm/yr) and decrease to the north and south to ~10 mm/yr (Fig. 2A). These north-south gradients in forearc motion promote oroclinal bending by imparting opposing shear strain on opposite limbs of the orocline.

Given the approximate spatial coincidence of the axial trace of the orocline with the slab arch hinge, we further suggest that oroclinal

bending at Cascadia results from decoupling between margin-normal strain accommodated on the megathrust and slab strike-parallel strain taken up within the forearc. The trench-parallel component of relative plate motion is right lateral in sense south of the Olympic Peninsula and decreases to near zero north of the peninsula, without a change in the sense of obliquity (Fig. 4). However, the component of relative plate motion parallel to slab strike at ~30–50 km depth on the plate interface changes sense across the slab arch hinge, near the axial trace of the orocline (Fig. 4). Maximum horizontal compressive stress directions (S_{Hmax}) within the upper-plate crust, calculated from crustal earthquake focal mechanisms and borehole breakouts (Balfour et al., 2011; Heidbach et al., 2016), trend subparallel to slab strike and fan around the Olympic Peninsula in a concave-outboard shape (Fig. 4). Quaternary-active faults surrounding the core of the orocline have slip senses consistent with the kinematics predicted by this crustal stress field (Fig. 4, upper inset). These observations support the idea that forearc strain is dominated by slab strike-parallel stresses that promote opposing senses of shear and rotation on the orocline limbs.

LONG-LIVED (>10 M.Y.) OROCLINAL BENDING AND ITS RELATIONSHIP TO MARGIN CONCAVITY

The alignment (within ~20 km distance and ~10°–20° trend) of the geologically (Fig. 2B) and geodetically defined (Fig. 3) axial traces of the orocline suggests that the processes that accommodate oroclinal bending, including flexural slip on the limbs and shortening, uplift, and escape within the orocline core, have persisted at the same position within the upper plate over a relatively long (>10 m.y.) period of time. Assuming that the Olympic orocline has persisted since at least the Miocene onset of uplift of the Olympic Mountains at ca. 18 Ma (Brandon et al., 1998), the paleomagnetic rotations measured in Eocene rocks imply an average rotation rate of $1.251 \pm 1.0\%$ m.y., which is comparable to the geodetically derived contemporary average rotation rate of $10.961 \pm 0.85\%$ m.y. (Fig. 3; Table DR1). If oroclinal bending at Cascadia is intrinsically related to both slab geometry and subduction obliquity, as we suggest, these results imply that the current along-strike variations in slab geometry and subduction obliquity have remained in the same position relative to the upper plate since at least the Miocene.

Although the initiation of bending may have been influenced by past margin geometry or the subduction of an indenter, we suggest that the concave-outboard geometry at Cascadia can be sustained by these persistent along-strike variations in slab geometry and subduction obliquity alone. The crustal processes associated with oroclinal bending should result in relative arcward

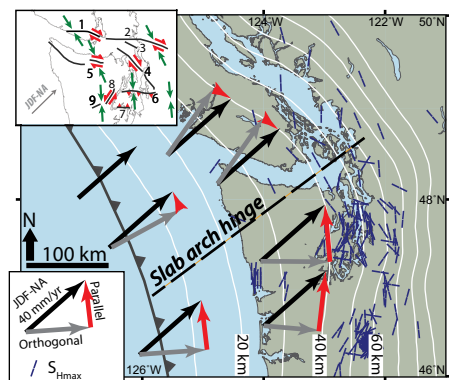


Figure 4. Along-strike changes in subduction obliquity with respect to Juan de Fuca slab depth contours (white lines; McCrory et al., 2012), and horizontal compressive stress (S_{Hmax}) directions in the upper plate (Balfour et al., 2011; Heidbach et al., 2016). Black arrows: Juan de Fuca–North America (JDF-NA) relative plate motion; gray and red arrows: slab contour-normal and slab contour-parallel components of motion, respectively (see lower inset) (MORVEL model; DeMets et al., 2010). Upper inset: Simplified S_{Hmax} orientations (green arrows) relative to strike and known kinematics of active faults (fault numbering and references as in Fig. 2).

motion of the trench along the axial trace of the orocline, and relative seaward rotation of the trench in the orocline limbs. Assuming that rates of influx of accreted sediment and outflux of eroded sediment at the trench are in equilibrium at all points along strike (Pazzaglia and Brandon, 2001), the long-lived opposing shear strain inherent to the geometry and kinematics of the plate margin will maintain a trench concavity that aligns with the axial trace of the orocline, as observed in Cascadia.

Similar patterns of vertical-axis rotations, crustal shortening, relative plate motions, and slab geometry occur at the apex of the ~5000-km-long concave-outboard bend in the South American margin near Bolivia. Much like at Cascadia, long-lived and ongoing bending of the Bolivian orocline is recorded by paleomagnetic and GNSS vertical-axis rotations, both of which are opposite in sign and similar in rate on each orocline limb (Allmendinger et al., 2005a). The axial trace of the Bolivian orocline also corresponds with both a convex-upward slab arch in the subducting Nazca plate (Hayes et al., 2012) and a reversal in subduction obliquity at the apex of the margin concavity. Kinematics of Pliocene–Quaternary faulting (Allmendinger et al., 2005b) and modelling of GNSS data (Bevis et al., 2001) suggest that margin-parallel shortening occurs on margin-normal faults in the core of the Bolivian orocline, in a similar manner as at Cascadia. These similarities indicate that persistent oroclinal bending, related to slab geometry and subduction obliquity, may be a common characteristic of the upper plate at concave-outboard convergent margins.

CONCLUSIONS

We demonstrate, for the first time, that active bending of the Olympic orocline has persisted from at least the Miocene (ca. 18 Ma) to the present, and is accommodated by flexural slip on the orocline limbs and crustal shortening, exhumation, and lateral escape within the orocline core. We observe a subparallelism in map view between the axial trace of the orocline and the hinge line of an arch in the subducting slab, indicating that orocline bending is maintained by opposing senses of shear on the orocline limbs due to variations in plate-boundary tractions intrinsic to the geometry of the slab arch. Our results imply that the Cascadia margin, much like at Bolivia, is an example of a long-lived orocline that has led to the development of a long-wavelength concave-outboard margin concavity, without the need for the subduction of an indenter in the present.

ACKNOWLEDGMENTS

Stephane Mazzotti provided Fortran code for computing rotations from GNSS velocity data. Figures were created with Generic Mapping Tools software (Wessel et al., 2013). We thank Yvette Kuiper, Jack Loveless, Dennis Brown, and an anonymous reviewer for comments that helped improve this manuscript. This research was partially supported by a University of Victoria (Canada) Jamie Cassels Undergraduate Research Award to Finley, and by U.S. National Science Foundation grants EAR-1756834 and EAR-1756943.

REFERENCES CITED

Allmendinger, R.W., Smalley, R., Jr., Bevis, M., Caprio, H., and Brooks, B., 2005a, Bending the Bolivian orocline in real time: *Geology*, v. 33, p. 905–908, <https://doi.org/10.1130/G21779.1>.

Allmendinger, R.W., González, G., Yu, J., Hoke, G., and Isacks, B., 2005b, Trench-parallel shortening in the Northern Chilean Forearc: Tectonic and climatic implications: *Bulletin of the Geological Society of America*, v. 117, p. 89–104, <https://doi.org/10.1130/B25505.1>.

Balfour, N.J., Cassidy, J.F., Dosso, S.E., and Mazzotti, S., 2011, Mapping crustal stress and strain in southwest British Columbia: *Journal of Geophysical Research*, v. 116, B03314, <https://doi.org/10.1029/2010JB008003>.

Beck, M.E., Jr., and Engebretson, D.C., 1982, Paleomagnetism of small basalt exposures in the west Puget Sound area, Washington, and speculations on the accretionary origin of the Olympic Mountains: *Journal of Geophysical Research*, v. 87, p. 3755–3760, <https://doi.org/10.1029/JB087iB05p03755>.

Bendick, R., and Ehlers, T.A., 2014, Extreme localized exhumation at syntaxes initiated by subduction zone geometry: *Geophysical Research Letters*, v. 41, p. 5861–5867, <https://doi.org/10.1002/2014GL061026>.

Bevis, M., Kendrick, E., Smalley, R., Jr., Brooks, B., Allmendinger, R., and Isacks, B., 2001, On the strength of interplate coupling and the rate of back arc convergence in the central Andes: An analysis of the interseismic velocity field: *Geochemistry Geophysics Geosystems*, v. 2, 1067, <https://doi.org/10.1029/2001GC000198>.

Bobillo-Ares, N.C., Bastida, F., and Aller, J., 2000, On tangential longitudinal strain folding: *Tectonophysics*, v. 319, p. 53–68, [https://doi.org/10.1016/S0040-1951\(00\)00026-3](https://doi.org/10.1016/S0040-1951(00)00026-3).

Brandon, M.T., and Calderwood, A.R., 1990, High-pressure metamorphism and uplift of the Olympic subduction complex: *Geology*, v. 18, p. 1252–1255, [https://doi.org/10.1130/0091-7613\(1990\)018<1252:HPMAUO>2.3.CO;2](https://doi.org/10.1130/0091-7613(1990)018<1252:HPMAUO>2.3.CO;2).

Brandon, M.T., Roden-Tice, M.K., and Garver, J.I., 1998, Late Cenozoic exhumation of the Cascadia accretionary wedge in the Olympic Mountains, northwest Washington State: *Geological Society of America Bulletin*, v. 110, p. 985–1009, [https://doi.org/10.1130/0016-7606\(1998\)110<0985:LCEOTC>2.3.CO;2](https://doi.org/10.1130/0016-7606(1998)110<0985:LCEOTC>2.3.CO;2).

Cady, W.M., 1975, Tectonic setting of the Tertiary volcanic rocks of the Olympic Peninsula, Washington: *Journal of Research of the U.S. Geological Survey*, v. 3, p. 573–582.

Carey, S.W., 1955, The orocline concept in geotectonics—Part I: Papers and Proceedings of the Royal Society of Tasmania, v. 89, p. 255–288.

DeMets, C., Gordon, R.G., and Argus, D.F., 2010, Geologically current plate motions: *Geophysical Journal International*, v. 181, p. 1–80, <https://doi.org/10.1111/j.1365-246X.2009.04491.x>.

Dietrich, D., 1989, Fold-axis parallel extension in an arcuate fold- and thrust belt: The case of the Helvetic nappes: *Tectonophysics*, v. 170, p. 183–212, [https://doi.org/10.1016/0040-1951\(89\)90271-0](https://doi.org/10.1016/0040-1951(89)90271-0).

Donath, F.A., and Parker, R.B., 1964, Folds and faulting: *Geological Society of America Bulletin*, v. 75, p. 45–62, [https://doi.org/10.1130/0016-7606\(1964\)75\[45:FAF\]2.0.CO;2](https://doi.org/10.1130/0016-7606(1964)75[45:FAF]2.0.CO;2).

Eldredge, S., Bachtadse, V., and Van Der Voo, R., 1985, Paleomagnetism and the orocline hypothesis: *Tectonophysics*, v. 119, p. 153–179, [https://doi.org/10.1016/0040-1951\(85\)90037-X](https://doi.org/10.1016/0040-1951(85)90037-X).

Hayes, G.P., Wald, D.J., and Johnson, R.L., 2012, Slab1.0: A three-dimensional model of global subduction zone geometries: *Journal of Geophysical Research*, v. 117, B01302, <https://doi.org/10.1029/2011JB008524>.

Heidbach, O., Rajabi, M., Reiter, K., Ziegler, M., and WSM Team, 2016, World Stress Map Database Release 2016: Potsdam, Germany, GFZ Data Services, <https://doi.org/10.5880/WSM.2016.001>.

Johnston, S.T., and Acton, S., 2003, The Eocene Southern Vancouver Island Orocline—A response to seamount accretion and the cause of fold-and-thrust belt and extensional basin formation: *Tectonophysics*, v. 365, p. 165–183, [https://doi.org/10.1016/S0040-1951\(03\)00021-0](https://doi.org/10.1016/S0040-1951(03)00021-0).

Li, G., Liu, Y., Regalla, C., and Morell, K.D., 2018, Seismicity relocation and fault structure near the Leech River fault zone, southern Vancouver Island: *Journal of Geophysical Research: Solid Earth*, v. 123, p. 2841–2855, <https://doi.org/10.1002/2017JB015021>.

Mahadevan, L., Bendick, R., and Liang, H., 2010, Why subduction zones are curved: *Tectonics*, v. 29, TC6002, <https://doi.org/10.1029/2010TC002720>.

Marshak, S., 2004, Salients, recesses, arcs, oroclines, and syntaxes—A review of ideas concerning the formation of map-view curves in fold-thrust belts, in McClay, K.R., ed., *Thrust Tectonics and Hydrocarbon Systems: American Association of Petroleum Geologists Memoir 82*, p. 131–156, <https://doi.org/10.1306/M82813C9>.

Mazzotti, S., Dragert, H., Hyndman, R.D., Miller, M.M., and Henton, J.A., 2002, GPS deformation in a region of high crustal seismicity: N. Cascadia forearc: *Earth and Planetary Science Letters*, v. 198, p. 41–48, [https://doi.org/10.1016/S0012-821X\(02\)00520-4](https://doi.org/10.1016/S0012-821X(02)00520-4).

Mazzotti, S., Leonard, L.J., Cassidy, J.F., Rogers, G.C., and Halchuk, S., 2011, Seismic hazard in western Canada from GPS strain rates vs. earthquake catalog: *Journal of Geophysical Research*, v. 116, B12310, <https://doi.org/10.1029/2011JB008213>.

McCaffrey, R., King, R.W., Payne, S.J., and Lancaster, M., 2013, Active tectonics of northwestern U.S. inferred from GPS-derived surface velocities: *Journal of Geophysical Research: Solid Earth*, v. 118, p. 709–723, <https://doi.org/10.1029/2012JB009473>.

McCrory, P.A., Blair, J.L., Waldhauser, F., and Oppenheimer, D.H., 2012, Juan de Fuca slab geometry and its relation to Wadati-Benioff zone seismicity: *Journal of Geophysical Research*, v. 117, B09306, <https://doi.org/10.1029/2012JB009407>.

Morell, K.D., Regalla, C., Leonard, L.J., Amos, C., and Levson, V., 2017, Quaternary rupture of a crustal fault beneath Victoria, British Columbia, Canada: *GSA Today*, v. 27, no. 3, p. 4–10, <https://doi.org/10.1130/GSATG291A.1>.

Nelson, A.R., Personius, S.F., Wells, R.E., Schermer, E.R., Bradley, L.-A., Buck, J., and Reitman, N., 2017, Holocene earthquakes of magnitude 7 during westward escape of the Olympic Mountains, Washington: *Bulletin of the Seismological Society of America*, v. 107, p. 2394–2415, <https://doi.org/10.1785/02160323>.

Pazzaglia, F.J., and Brandon, M.T., 2001, A fluvial record of long-term steady-state uplift and erosion across the Cascadia forearc high, western Washington State: *American Journal of Science*, v. 301, p. 385–431, <https://doi.org/10.2475/ajs.301.4.5.385>.

Prothero, D.R., Draus, E., Cockburn, T.C., and Nesbitt, E.A., 2008, Paleomagnetism and counterclockwise tectonic rotation of the upper Oligocene Sooke Formation, southern Vancouver Island, British Columbia: *Canadian Journal of Earth Sciences*, v. 45, p. 499–507, <https://doi.org/10.1139/E08-012>.

Silver, E.A., Reed, D.L., Tagudin, J.E., and Heil, D.J., 1990, Implications of the north and south Panama thrust belts for the origin of the Panama orocline: *Tectonics*, v. 9, p. 261–281, <https://doi.org/10.1029/TC009i002p00261>.

Wang, K., Wells, R., Mazzotti, S., Hyndman, R.D., and Sagiya, T., 2003, A revised dislocation model of interseismic deformation of the Cascadia subduction zone: *Journal of Geophysical Research*, v. 108, 2026, <https://doi.org/10.1029/2001JB001227>.

Warnock, A.C., Burmester, R.F., and Engebretson, D.C., 1993, Paleomagnetism and tectonics of the Crescent Formation, northern Olympic Mountains, Washington: *Journal of Geophysical Research*, v. 98, p. 11729–11741, <https://doi.org/10.1029/93JB00709>.

Washington Geological Survey, 2017, Surface geology, 1:24,000—GIS data, September 2017: Washington Geological Survey Digital Data Series DS-10, version 3.0.

Wessel, P., Smith, W.H.F., Scharroo, R., Luis, J., and Wobbe, F., 2013, Generic Mapping Tools: Improved version released: *Eos (Transactions, American Geophysical Union)*, v. 94, p. 409–410, <https://doi.org/10.1002/2013EO450001>.

Yu, G., Wesnousky, S.G., and Ekström, G., 1993, Slip partitioning along major convergent plate boundaries: *Pure and Applied Geophysics*, v. 140, p. 183–210, <https://doi.org/10.1007/BF00879405>.

Printed in USA